

# Statistical Effects of Frequency Instability on Continuous Monitoring of Active and Reactive Power

DIEGO BELLAN

Department of Electronics, Information and Bioengineering  
Politecnico di Milano  
Piazza Leonardo da Vinci, 32, 20133 Milano  
ITALY

*Abstract:* - This paper provides an approximate analytical approach leading to the statistical characterization of the electric active/reactive power related to the harmonics in the real-time monitoring of a power system affected by frequency instability. The effect of additive noise is also included in the analysis. Frequency instability of voltage and current waveforms is modeled as a random variable ranging within a given frequency interval. Propagation of both the uncertainty sources through the whole measurement process based on analog-to-digital conversion and discrete Fourier transform is investigated. Power evaluation is performed by proper multiplication of waveforms spectra. In fact, the requirement of real-time monitoring prevents the use of sophisticated algorithms to cope with the frequency change before spectra multiplication. Analytical expressions taking into account the weighting function used against spectral leakage are derived for the bias and the standard deviation of the measured power.

*Key-Words:* - Power measurement; power quality; frequency instability; additive noise; discrete Fourier transform; statistical techniques.

## 1 Introduction

Modern electrical power systems are characterized by increasing complexity mainly due to the so-called distributed generation (DG) and to the widespread use of non-linear loads. In particular, the use of time-varying non-linear loads requires a continuous real-time monitoring of the harmonic content in the waveforms spectra for power quality purposes. It is well-known, however, that one of the drawbacks of DG is frequency instability/inaccuracy of the generated waveforms. Therefore, as the main objective of this paper, it is of paramount importance to investigate the effect of frequency instability on the power measurements performed by digital techniques based on analog-to-digital (A/D) conversion of the waveforms and the discrete Fourier transform (DFT) usually evaluated through the fast Fourier transform (FFT) [1]. The impact of additive noise is also investigated in order to attain a complete characterization of the measurement process. In the literature a few attempts have been made along this direction. In [2] only the effect of additive noise was taken into account with respect to measurement of the average power. Active and reactive powers at harmonic components were not investigated. In other papers (e.g., see [3]-[5]) sophisticated algorithms were proposed to face the

problem of unknown frequency. However, this approach is not suited to the need of a continuous real-time monitoring.

The paper is organized as follows. The problem statement is provided in Section 2. The mathematical derivations leading to the statistical characterization of the measured harmonic power are provided in Section 3. Numerical validation of the analytical results is given in Section 4. Final remarks are provided in Section 5.

## 2 Problem Statement

Power measurements under non-sinusoidal conditions can be effectively performed by resorting to digital instrumentation based on A/D conversion of voltage and current waveforms, and time-to-frequency transformation through the DFT (with the efficient FFT algorithm). Thus, active and reactive power at each frequency of interest can be readily evaluated by processing the relevant spectral lines.

Two main sources of uncertainty can be identified in the measurement process outlined above. First, the fundamental frequency of voltage/current waveforms is typically affected by random instability. It means that by repeating the measurement process, slightly different values of

the waveforms fundamental frequency must be expected. Such frequency instability is of course emphasized for harmonic components. When the DFT is applied, the lack of synchronism between the waveforms fundamental frequency and the sampling frequency (i.e., non-coherent sampling) will result in increased uncertainty in the power measurements. The second main source of uncertainty is additive noise. Indeed, voltage/current waveforms are always affected by additive noise which propagates through A/D conversion and DFT transformation, yielding noisy spectral lines. It is expected that the impact of additive noise is larger as the amplitude of the involved harmonic spectral lines decreases. Therefore, the resulting power evaluations should be properly characterized in statistical terms by treating each power estimate as a random variable (RV).

The time-domain voltage/current waveforms are modelled as a sum of  $N$  sine waves and additive zero-mean independent noise:

$$v(t) = \sqrt{2} \sum_{h=1}^N V_h \cos(2\pi f_h t + \varphi_h) + n_v(t) \quad (1)$$

$$i(t) = \sqrt{2} \sum_{h=1}^N I_h \cos(2\pi f_h t + \vartheta_h) + n_i(t) \quad (2)$$

After A/D conversion of (1)-(2) with sampling frequency  $f_s$ , and weighted time-windowing ( $N_s$  samples in length) against spectral leakage [4], the DFT transform provides the estimates of the complex Fourier coefficients:

$$\hat{V}_n = \frac{\sqrt{2}}{N_s \text{NPSG}} \sum_{k=0}^{N_s-1} v[k] w[k] \exp(-j2\pi kn/N_s), \quad (3)$$

$$\hat{I}_n = \frac{\sqrt{2}}{N_s \text{NPSG}} \sum_{k=0}^{N_s-1} i[k] w[k] \exp(-j2\pi kn/N_s), \quad (4)$$

where  $w[k]$  is the selected time window characterized by the related Normalized Peak Signal Gain NPSG (see Tab. I where three examples of commonly used windows are reported with the parameters exploited in this paper). The frequency index  $n$  is related to the frequency index  $h$  in (1)-(2) by  $n \times \Delta f = f_h$ , where  $\Delta f = f_s/N_s$  is the DFT frequency resolution. Under non-coherent sampling, the relation  $n \times \Delta f = f_h$  is intended as an approximate relation where  $n$  is the index such that  $n \times \Delta f$  is the discrete frequency closest to  $f_h$ .

The estimates of the active and reactive power are derived from (3)-(4) as

$$\hat{P}_h = |\hat{V}_h| |\hat{I}_h| \cos(\arg \hat{V}_h - \arg \hat{I}_h), \quad (5)$$

$$h = 1, \dots, N \quad f_h \cong n \times \Delta f$$

$$\hat{Q}_h = |\hat{V}_h| |\hat{I}_h| \sin(\arg \hat{V}_h - \arg \hat{I}_h), \quad (6)$$

$$h = 1, \dots, N \quad f_h \cong n \times \Delta f$$

It is worth noticing that each of the RVs  $\{\hat{P}_h, \hat{Q}_h\}_{h=1}^N$  defined by the transformations (5) and (6) is given as a function of four RVs  $\{|\hat{V}_h|, |\hat{I}_h|, \arg \hat{V}_h, \arg \hat{I}_h\}$  for which statistical uncorrelation cannot be assumed. Indeed, it is well known that both  $|\hat{V}_h|$  and  $\arg \hat{V}_h$  are obtained by combining the real and the imaginary parts of the relevant DFT coefficient  $\hat{V}_h$ , and the same is true for  $|\hat{I}_h|$  and  $\arg \hat{I}_h$  with respect to the DFT coefficient  $\hat{I}_h$ . It follows that the analytical derivation of the statistical properties of the RVs  $\{\hat{P}_h, \hat{Q}_h\}_{h=1}^N$  given in the form (5) and (6) cannot be straightforward. In the next Section an alternative form for (5) and (6) will be provided, such that the statistical characterization of active and reactive power can be analytically derived through a straightforward approach.

### 3 Mathematical Derivations

In this Section the mathematical derivations will be performed with reference to the active power only. Similar derivations could be performed for the reactive power. Moreover, for the sake of simplicity, the frequency index  $h$  in (5) will be dropped since the proposed approach holds for each specific frequency  $f_h$ .

The two main sources of uncertainty outlined in Section 2 are analyzed in the following subsections.

#### 3.1 Frequency Instability

If the frequency  $f$  of a sinusoidal component in the voltage/current waveform does not equal one of the DFT discrete frequencies (i.e., the integer multiples of the frequency resolution  $\Delta f$ ), the related spectral-line magnitude does not take its ideal value. In fact, in this case (i.e., the non-coherent sampling condition) the spectral line magnitude is weighted by the Fourier transform of the time window  $w[k]$  used in (3)-(4) against spectral leakage. An approximate methodology is here introduced, consisting in the approximation of the frequency-domain behavior of each specific window by a parabolic function obtained by setting the constraint provided by the window Scallop Loss (SL) (see Fig. 1), i.e., the maximum attenuation introduced by the window at the edges  $\pm \Delta f/2$  of each DFT bin [6]. From Fig. 1, assuming the  $n$ -th DFT frequency bin as the origin of the frequency axis, the normalized

attenuation introduced by the window on a waveform spectral line can be readily obtained:

$$y \cong 1 - af^2 = 1 - \frac{4(1-SL)}{\Delta f^2} f^2 \quad (7)$$

Such attenuation is applied to both the voltage and the current spectral lines at the frequency  $f$ . Therefore, by defining

$$z = y^2 \quad (8)$$

the active power in (5) can be rewritten as

$$\hat{P} = z|\bar{V}||\bar{I}|\cos(\arg\hat{V} - \arg\hat{I}) \quad (9)$$

where  $|\bar{V}|$  and  $|\bar{I}|$  denote the non-weighted frequency-centered spectral lines.

The frequency  $f$  will be treated as a RV uniformly distributed within an interval  $df$  centered on the DFT frequency bin  $n \times \Delta f$  (see Fig. 1). It follows that also  $z$  is a RV whose mean value and variance can be estimated using an approximate approach based on a Taylor series expansion [7]-[8]:

$$\mu_z \cong 1 - \frac{2}{3}(1 - SL) \left(\frac{df}{\Delta f}\right)^2 \quad (10)$$

$$\sigma_z^2 \cong 0.36(1 - SL)^2 \left(\frac{df}{\Delta f}\right)^4 \quad (11)$$

### 3.2 Additive Noise

By using a well-known trigonometric identity, the active power (9) can be rewritten as

$$\begin{aligned} \hat{P} &= z|\bar{V}| \cos(\arg\hat{V}) |\bar{I}| \cos(\arg\hat{I}) \\ &+ z|\bar{V}| \sin(\arg\hat{V}) |\bar{I}| \sin(\arg\hat{I}) = \quad (12) \\ &= z\text{Re}\{\bar{V}\}\text{Re}\{\bar{I}\} + z\text{Im}\{\bar{V}\}\text{Im}\{\bar{I}\} \end{aligned}$$

In the literature it has been shown that the real and the imaginary parts of a DFT coefficient of a noisy waveform can be treated as Gaussian uncorrelated RVs, with mean values equal to the noise-free mean values, and variances given by [2]

$$\sigma^2 = \frac{1}{N_s} \sigma_n^2 \text{ENBW} \quad (13)$$

where  $\sigma_n^2$  is the variance of the additive input noise, and ENBW is the Equivalent Noise Bandwidth of the selected time window.

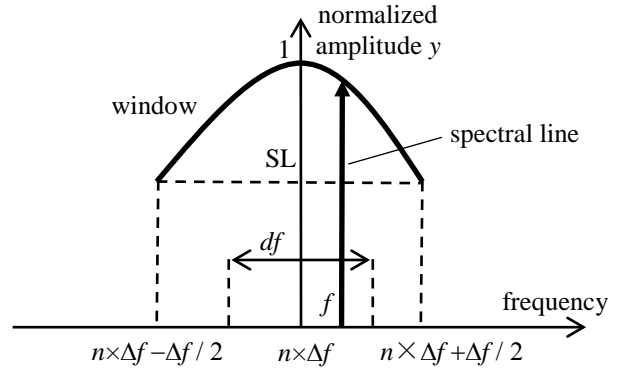


Fig. 1. Spectral line weighted by the frequency-domain window.

Therefore, for the real and the imaginary parts of the voltage DFT coefficients we have:

$$\sigma_V^2 = \frac{1}{N_s} \sigma_{n_v}^2 \text{ENBW} \quad (14)$$

whereas for the real and imaginary parts of the current DFT coefficients we have:

$$\sigma_I^2 = \frac{1}{N_s} \sigma_{n_i}^2 \text{ENBW} \quad (15)$$

### 3.3 Mean Value and Variance Estimates

The active power in (12) is a RV given as a function of five independent RVs whose mean values and variances have been derived in the previous subsections. Therefore, the mean value and the variance of  $\hat{P}$  can be obtained by means of the Taylor expansion approach already used above. The first-order partial derivatives can be readily evaluated from (12), whereas the second-order derivatives are all zero. Thus, the mean value of  $\hat{P}$  is given by:

$$\mu_{\hat{P}} \cong \mu_z P = \left[1 - \frac{2}{3}(1 - SL) \left(\frac{df}{\Delta f}\right)^2\right] P \quad (16)$$

which allows the evaluation of the normalized bias in the active power measurement:

$$b_P = \frac{\mu_{\hat{P}} - P}{P} = -\frac{2}{3}(1 - SL) \left(\frac{df}{\Delta f}\right)^2 \quad (17)$$

and the variance is given by:

$$\sigma_{\hat{P}}^2 \cong \sigma_z^2 P^2 + \mu_z^2 (\sigma_V^2 I^2 + \sigma_I^2 V^2) =$$

$$= 0.36(1 - SL)^2 \left(\frac{df}{\Delta f}\right)^2 P^2 + \left[1 - \frac{2}{3}(1 - SL) \left(\frac{df}{\Delta f}\right)^2\right]^2 \frac{\text{ENBW}}{N_s} (\sigma_{n_v}^2 I^2 + \sigma_{n_i}^2 V^2) \quad (18)$$

TABLE I.  
SOME FIGURES OF MERIT OF THREE COMMON WINDOWS.

Window	NPSG	ENBW	SL [dB]	SL
Rect.	1	1	3.92	0.637
Tukey ( $\alpha=0.5$ )	0.75	1.22	2.24	0.773
Hann	0.50	1.50	1.42	0.849

such that the normalized standard deviation can be written:

$$\frac{\sigma_P}{P} = \sqrt{0.36(1 - SL)^2 \left(\frac{df}{\Delta f}\right)^2 + \left[1 - \frac{2}{3}(1 - SL) \left(\frac{df}{\Delta f}\right)^2\right]^2 \frac{\text{ENBW}}{N_s} \frac{\sigma_{n_v}^2 + \sigma_{n_i}^2}{\cos^2(\varphi - \vartheta)}} \quad (19)$$

It is interesting to notice in (19) two kinds of additive contributions. The first term is strictly related to the frequency uncertainty  $df/\Delta f$  and the SL of the window. The second term includes also the contribution of the noise-to-signal ratios  $\sigma_{n_v}^2/V^2$  and  $\sigma_{n_i}^2/I^2$ , showing that higher-order low-amplitude harmonics result in larger uncertainty. The total noise-to-signal ratio is divided by the squared power factor  $\cos^2(\varphi - \vartheta)$  which in turn can emphasize such contribution for small power factors. Moreover, as expected, the total noise-to-signal ratio is weighted by the ENBW parameter of the window, while the action of the number of samples  $N_s$  is distributing the noise power over the DFT frequency bins such that the noise impact decreases as  $N_s$  increases. Finally, it can be easily shown that the above results hold also for the reactive power.

#### 4 Numerical Simulations

The analytical results derived in Section 3 have been validated by resorting to numerical simulation of the whole measurement process. According to (1)-(2), voltage and current waveforms consisting of three harmonic components have been selected such that  $f_1 = 50$  Hz,  $f_3 = 3f_1$ ,  $f_5 = 5f_1$ . The voltage and current rms values have been selected as  $V_1 = 1$ ,  $V_3 = 0.1$ ,  $V_5 = 0.04$ ,  $I_1 = 0.5$ ,  $I_3 = 0.1$ ,  $I_5 = 0.02$ . Phase angles 1 and 3 have been selected at random, while phase angles 5 have been given specific values since the analytical result (19) has been tested for the fifth harmonic component. Time-domain additive zero-mean Gaussian noise has been

considered with  $\sigma_{n_v} = \sigma_{n_i} = 0.04$ . Sampling has been performed such that 10 periods of the fundamental component are acquired, i.e., a 200 ms measurement window were taken. The selection of the number of samples  $N_s$  defines the corresponding sampling frequency. By assuming  $N_s = 2^{12}$  the corresponding sampling

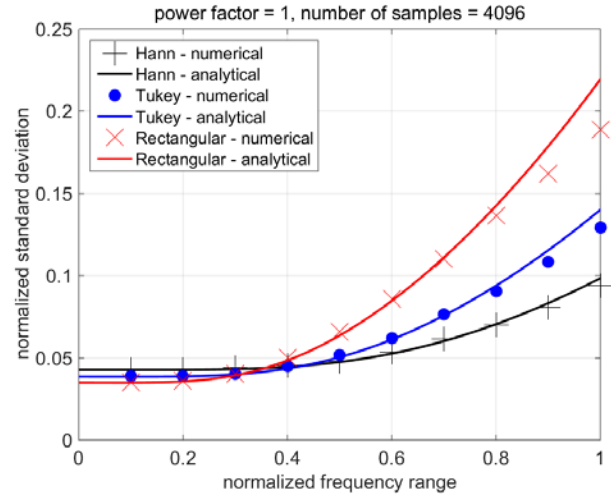


Fig. 2. Comparison between analytical (solid lines) and numerical (markers) estimates of the normalized standard deviation of  $P_s$  (see (19)) as a function of the normalized frequency range  $df/\Delta f$  for three different windows.

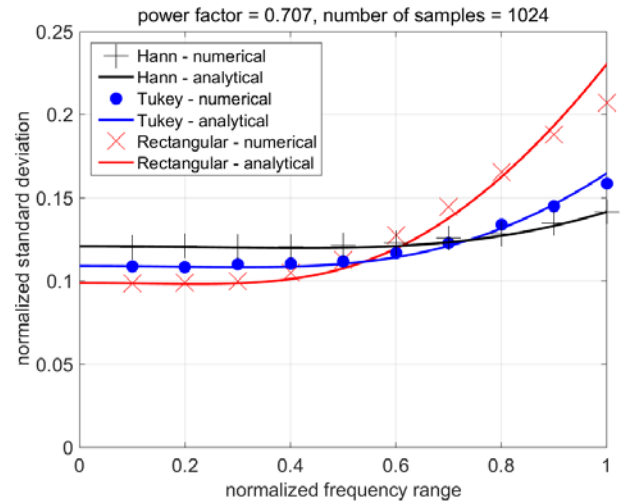


Fig. 3. Same as Fig. 2 but with decreased power factor and number of samples.

frequency is  $f_s = 20.48$  kHz, and the related frequency resolution is  $\Delta f = 5$  Hz. A repeated run analysis ( $10^4$  runs to estimate each average value) has been performed by assuming  $f_1$  taking random values with uniform distribution within a frequency range  $df$  centered on the nominal frequency 50 Hz. It is worth noticing that a frequency deviation  $df$  in the fundamental component results in a frequency

deviation  $3df$  in the third harmonic, and  $5df$  in the fifth harmonic. In the following, analytical results (17) and (19) have been validated for the fifth harmonic. In fact, by assuming a maximum  $\frac{df}{\Delta f} = 0.2$  for the fundamental component, such normalized frequency range equals 1 for the fifth harmonic. Moreover, the effect of the noise part in (19) is emphasized when low-magnitude sine-waves are considered.

In Fig. 2 the normalized standard deviation (19) related to  $P_5$  is validated against the numerical simulations described above. The power factor  $\cos(\varphi_5 - \vartheta_5)$  has been selected equal to 1. The contribution of noise in (19) is mainly relevant to the first part of the curves, i.e., for small values of  $df/\Delta f$ .

In Fig. 3 the power factor was decreased to 0.707, and the number of samples was decreased to 1024. According to (19), decreasing of both the parameters emphasizes the contribution of noise clearly evident for small values of  $df/\Delta f$ .

## 5 Conclusion

Approximation of the frequency behavior of the window used against spectral leakage by a simple parabolic function, depending only on the parameter SL, provided analytical results in good agreement with numerical simulations. The proposed approach enables simple and straightforward statistical characterization of measured power affected by frequency instability and noise.

Future work will be devoted to extend the analytical results to different and possibly non-symmetrical statistical distributions for the frequency instability.

## References:

- [1] D. Bellan, Frequency Instability and Additive Noise Effects on Digital Power Measurements Under Non-Sinusoidal Conditions, in *Proc. 2014 6<sup>th</sup> IEEE Power India International Conference (PIICON)*, Delhi, India, Dec. 5-7, 2014, pp. 1-5.
- [2] P. Carbone and D. Petri, Average power estimation under nonsinusoidal conditions, *IEEE Trans. on Instrum. Meas.*, vol. 49, no. 2, April 2000, pp. 333-336.
- [3] D. Agrez, Active power estimation in the non-coherent sampling: a comparative study, in *Proc. of IMTC 2005 – Instrum. Meas. Technology Conference*, Ottawa, Canada, 17-19 May, 2005, pp. 720-725.
- [4] M. H. Wang and Y. Z. Sun, A practical, precise method for frequency tracking and phasor estimation, *IEEE Trans. on Power Delivery*, vol. 19, no. 4, Oct. 2004, pp. 1547–1552.
- [5] M. Wang and Y. Sun, A practical method to improve phasor and power measurement accuracy of DFT algorithm, *IEEE Trans. on Power Delivery*, vol. 21, no. 3, July 2006, pp. 1054-1062.
- [6] F. J. Harris, On the use of windows for harmonic analysis with the discrete Fourier transform, *Proc. of the IEEE*, vol. 66, 1978, pp. 51-83.
- [7] D. Bellan, Statistical characterization of harmonic emissions in power supply systems, *International Review of Electrical Engineering*, vol. 9, no. 4, 2014, pp. 803-810.
- [8] D. Bellan and S. A. Pignari, Statistical superposition of crosstalk effects in cable bundles, *China Communications*, Nov. 2013, pp. 119-128.

## Creative Commons Attribution License 4.0 (Attribution 4.0 International, CC BY 4.0)

This article is published under the terms of the Creative Commons Attribution License 4.0  
[https://creativecommons.org/licenses/by/4.0/deed.en\\_US](https://creativecommons.org/licenses/by/4.0/deed.en_US)